

**Effect of chitosan on distearoylphosphatidylglycerol (DSPG)
films at air/water and liquid/liquid interfaces**

Journal:	<i>Biomacromolecules</i>
Manuscript ID:	Draft
Manuscript Type:	Article
Date Submitted by the Author:	n/a
Complete List of Authors:	Cámara, Candelaria; Facultad de Ciencias Químicas, Universidad Nacional de Córdoba, Fisicoquímica Colqui Quiroga, Monica; Facultad de Ciencias Químicas, Universidad Nacional de Córdoba, Fisicoquímica Wilke, Natalia; Facultad de Ciencias Químicas, Universidad Nacional de Córdoba, Química Biológica Jimenez-Kairuz, Alvaro; Facultad de Ciencias Químicas, Universidad Nacional de Córdoba, Farmacia Yudi, Lidia; Facultad de Ciencias Químicas, Universidad Nacional de Córdoba, Fisicoquímica

SCHOLARONE™
Manuscripts

Effect of chitosan on distearoylphosphatidylglycerol (DSPG) films at air/water and liquid/liquid interfaces

Candelaria I. Cámara^a, Mónica V. Colqui Quiroga^a, Natalia Wilke^b, Alvaro Jimenez-Kairuz^c
and Lidia M. Yudi^{a*}.

^a *Instituto de Investigaciones en Fisicoquímica de Córdoba (INFIQC- CONICET).
Departamento de Fisicoquímica, Facultad de Ciencias Químicas, Universidad Nacional de
Córdoba. Ala 1, Pabellón Argentina, Ciudad Universitaria, 5000 Córdoba, Argentina. Tel:
(+54) 0351- 4334169/ 80. Fax: (+54) 0351 - 4334188.*

^b *Centro de Investigaciones en Química Biológica de Córdoba (CIQUIBIC- CONICET),
Departamento de Química-Biologica, Facultad de Ciencias Químicas, Universidad Nacional
de Córdoba. Ala 1, Pabellón Argentina, Ciudad Universitaria, 5000 Córdoba, Argentina. Tel:
(+54) 0351- 4334171/68.*

^c *Departamento de Farmacia, Facultad de Ciencias Químicas, Universidad Nacional de
Córdoba, Haya de la Torre y medina Allende, Ciudad Universitaria, 5000 Córdoba,
Argentina. Tel: (+54) 0351- 4334163/27.*

*Corresponding author. E – mail: mjudi@fcq.unc.edu.ar

Abstract

The effect of chitosan on distearoylphosphatidylglycerol (DSPG) films was analyzed by cyclic voltammetry, surface pressure-area and surface potential –area isotherm and Brewster Angle Microscopy.

Experiments of cyclic voltammetry at a liquid/liquid interface demonstrated a blocking effect of DSPG to tetraethylammonium (TEA^+) cation transfer from the aqueous to the organic phase. This effect was reversed by the presence of chitosan, which modifies the film structure. Special emphasis was placed on the nature of the supporting aqueous electrolyte (LiCl or CaCl_2). In the presence of LiCl the permeability of the film increases when chitosan is present in the aqueous phase, minimizing the blocking effect of the film on TEA^+ transfer probably due to the presence of bare zones at the interface. Oppositely, in presence of Ca^{2+} , the enhancement of permeability was not observed, probably due to the impediment of chitosan to penetrate into the very tightly compacted film of DSPG. Electrochemical experiments were completed with viscosity measurements to explain the variation of diffusion coefficients for TEA^+ .

Langmuir isotherms for DSPG monolayers modified with chitosan, demonstrate that this polymer produces an expansion of the DSPG film and modifies the compression factor, for both electrolytes studied.

Images of Brewster angle microscopy evidence an increase in the optical thickness of the DSPG films in presence of chitosan indicating that the polymer interacts with DSPG molecules at low and high molecular areas.

Keywords: Chitosan, phospholipids monolayers, liquid/liquid interfaces, air/water interfaces, cyclic voltammetry, Langmuir isotherms.

1. Introduction

Chitin is a homopolymer of β (1-4)-linked N-acetyl-D-glucosamine and the second abundant natural polymer after cellulose. It is found in the exoskeleton of many invertebrates and in the cell walls of most fungi¹. Chitosan (Scheme 1), is a natural polyaminosaccharide^{2,3} obtained by N-deacetylation of chitin. It possesses multiple amino groups, which give a skeleton with high positive charge when dissolved in acid medium ($pK_a = 6.9$). The growing interest in the study of the chitosan chemistry is based on its properties of biocompatibility, biodegradability and low cytotoxicity^{3,4}. These features become this polymer an excellent candidate for medical applications. As a consequence of its important properties, chitosan has been used for a large number of applications including: chelating of heavy metal ions⁵⁻⁷, fat reducer agent⁸, drugs^{9,10} and gene delivery systems¹¹, bactericide agent¹² and blood coagulation¹³ among others.

Recent studies demonstrate that chitosan can interact with liposomes¹⁴, proteins¹⁵⁻¹⁷, lipids^{18,19} and biomembranes²⁰⁻²⁴, and emphasize the importance of understanding the nature of such interactions because most of the uses of chitosan involve the contact with cell membranes.

H. Parra-Barraza et al. investigated the influence of chitosan in the properties of cholesterol and stearic acid monolayers, demonstrating that this polyelectrolyte alters the rigidity of the monolayers²⁵. On the other hand, experiments of Langmuir and Langmuir-Blodgett isotherms and infrared microscopy²⁶ demonstrated that chitosan interacts with

1
2
3 dimyristoyl phosphatidic acid (DMPA) monolayers, causing expansion and decreasing the
4
5 monolayer elasticity. In that work, the authors propose a model in which chitosan interacts
6
7 with DMPA film via dipole and electrostatic interactions. Additionally, recent studies
8
9 reported by Silva et al. demonstrate that chitosan forms a complex with mucin in DMPA
10
11 monolayers, based on electrostatic interaction²⁷.
12
13
14

15 Electrochemical measurements applied to liquid-liquid interfaces modified by
16
17 different films have been carried out in the last decades with the aim of developing new
18
19 biomimetic membranes models. In this sense, the adsorption of lipid monolayer²⁸⁻³⁰,
20
21 proteins³¹, surfactants³² or polyelectrolyte³³ has been studied and the properties of these films
22
23 have been characterized by cyclic voltammetry, electrochemical impedance spectroscopy, and
24
25 surface tension measurements. One aspect of special interest has been the study of the
26
27 interaction or the complex formation between phospholipid monolayers and alkaline or
28
29 alkaline earth cations³⁴, trivalent cations³⁵, peptides³⁶ and different organic anions³⁷, with the
30
31 purpose of analyzing the blocking effect of these species on the monolayer structure. All
32
33 references listed above demonstrate that electrochemical techniques applied at the interface
34
35 between two immiscible electrolyte solutions (ITIES) are ideal to follow dynamic changes in
36
37 the lipid layer compactness and interfacial interactions at a hydrophobic / hydrophilic
38
39 boundary.
40
41
42
43
44
45

46 In previous papers we have studied the incorporation of anxiolytics drugs into the
47
48 phospholipid monolayers adsorbed at liquid/liquid interfaces³⁸⁻⁴². The results obtained
49
50 contribute to the knowledge of the non-specific interaction between these drugs and biological
51
52 membranes components, which is particularly important because their accumulation in
53
54 biomembranes alters the structural properties leading to collateral effects. The combination of
55
56 surface pressure -molecular area measurements and electrochemical experiments employing a
57
58
59
60

test cation such as tetraethyl ammonium (TEA^+) allowed us to evaluate the permeability and the compactness of the monolayer. In the present paper we studied the effect of chitosan on distearoyl phosphatidyl glycerol (DSPG) films formed at water/1,2-dichloroethane or at the air/water interfaces, employing different experimental setups and techniques such as viscosity measurements, surface pressure – molecular area and surface potential – molecular area isotherms, Brewster angle microscopy and cyclic voltammetry. Special emphasis is placed in the composition of the aqueous phase which contained LiCl or CaCl_2 as electrolytes that, in turn, modified the effect of chitosan on DSPG films.

2. Experimental

2.1. Materials and electrochemical cell

Cyclic voltammetry (CV), performed in a four-electrode system using a conventional glass cell of 0.16 cm^2 interfacial area, were conducted to characterize the film. Two platinum wires were used as counter electrodes and the reference electrodes were Ag/AgCl. The reference electrode in contact with the organic solution was immersed in an aqueous solution of $1.0 \times 10^{-2} \text{ M}$ tetraphenylarsonium chloride (TPAsCl, Aldrich). Potential values (ΔE) reported in this work are those which include $\Delta\phi^0_{\text{tr, TPAs}^+} = 0.364 \text{ V}$ for the transfer of the reference ion TPAs^+ .

The base electrolyte solution were $1.0 \times 10^{-2} \text{ M}$ MCl_z ($\text{M}^{z+} = \text{Ca}^{2+}, \text{Li}^+$) (p.a. grade) in ultra pure water and $1.0 \times 10^{-2} \text{ M}$ tetraphenyl arsonium dicarbollyl cobaltate (TPAsDCC) in 1,2-dichloroethane (DCE, Dorwill p.a.). TPAsDCC was prepared by metathesis of TPAsCl

and sodium dicarbollyl cobaltate (Aldrich p.a.). The pH of the aqueous solution was 3.00, adjusted with 2.00 % v/v acetic acid glacial (Baker Analyzed). In all experiments 1.00 mL of organic and 4.00 mL of aqueous phase were used to fill the cell. In other set of experiments, the organic phase was gelled. For this purpose, 10.00 % w/v HMW-PVC and 30 μ L of Dioctyl Sebacate (Química Olivos S.A. C.I) were added to 1.00 mL of organic phase and heated at 75 $^{\circ}$ C for 3 min.

The electrochemical cell used was as follows:

Ag	AgCl	TPAsCl	TPAsDCC	MCl _n	AgCl	Ag
		1×10^{-2} M	1×10^{-2} M	1×10^{-2} M		
		(w')	(o)	(w)		

Pure Chitosan (Sigma Aldrich, MW: 50-190 KDa, >75 % deacetylated) was added to the aqueous phase (w) in a concentration range from 0 to 1.00 % w/v.

Distearoylphosphatidylglycerol (DSPG) was of analytical grade (Sigma-Aldrich). A solution containing 0.80 mg/mL of DSPG in 1:2 methanol: chloroform was prepared. In order to form the lipid film, 50 μ L of DSPG solution were injected, using a Hamilton microsyringe, at the liquid/liquid interface after both phases were put in contact in the electrochemical cell. A time equal to 60 min after the injection of the lipid solution was required to obtain reproducible voltammetric response, indicating that a stable lipid film had been formed. As a consequence, all experiments were performed after this equilibration time at room temperature equal to 25 ± 1 $^{\circ}$ C. Temperature was controlled with a temperature/humidity monitor.

1
2
3 It is important to remark that at pH = 3.00 chitosan is positively charged while the
4 polar head groups of DSPG molecules at the interface are partially ionized with negative
5 charge.
6
7
8
9

10 11 12 **2.2. Cyclic Voltammetry (CV) experiments**

13
14
15
16
17 Voltammograms were carried out using an aqueous solution of 5×10^{-4} M
18 tetraethylammonium chloride (TEACl, Sigma). The cation TEA^+ was employed as a probe
19 ion, since it transfers from the aqueous to the organic phase according to a direct reversible
20 diffusion controlled mechanism³⁷. The comparison between the voltammetric profiles for
21 TEA^+ before and after injection of DSPG, in the absence and in the presence of chitosan
22 dissolved in the aqueous phase, allows us to evaluate the ion permeability of the monolayer.
23
24
25
26
27
28
29
30

31
32 CV experiments were performed using a four-electrode potentiostat with periodic
33 current interruption for automatic elimination of solution resistance. The voltage was changed
34 from 0.200 V to 0.750 V with a potential sweep generator (L y P Electrónica, Argentina).
35
36
37 Voltammograms were recorded employing a 10 bit computer board acquisition card
38 connected to a personal computer. Voltammograms with typical errors of $\pm 10\%$ in current
39 values were obtained.
40
41
42
43
44
45
46
47

48 **2.3. Viscosity Experiments**

49
50
51
52
53 Viscosity measurements were performed in a rotational viscotester (Haake Viscotester
54 VT500, Termo Scientificric, Karlsruhe, Ger.) equipped with standard sensors, MV cup and
55
56
57
58
59
60

MV2 cylinder, as measuring systems. Data were collected and analyzed using the specifics software VT500, 3.01 version.

The apparent viscosity (η) was calculated from the linear portion of flow curves, obtained at shear rates ranging from 10 s^{-1} to 550 s^{-1} . All measurements were carried out at 25°C . Three replicates were tested for each sample and three measurements were performed for each replicate.

The composition of the aqueous solutions analyzed was: $1.0 \times 10^{-2} \text{ M LiCl}$, $2.00 \% \text{ v/v}$ acetic acid and chitosan in a concentration range from $0 \% \text{ w/v}$ to $1.00 \% \text{ w/v}$, $\text{pH} = 3.00$. The solutions were prepared from a $2.00\% \text{ w/v}$ chitosan stock solution.

2.4. Langmuir monolayers

2.4.1 Surface Pressure - molecular area isotherms

Surface pressure - molecular area isotherms were recorded with a mini-trough II from KSV Instruments Ltd. (Helsinki, Finland). The surface tension was measure using the Wilhelmy plate method with a platinum plate.

The aqueous subphase, contained in a Teflon trough ($364 \text{ mm} \times 75 \text{ mm}$ effective film area), was $1.0 \times 10^{-2} \text{ M MCl}_z$ ($\text{M}^{z+} = \text{Ca}^{2+}, \text{Li}^{+}$), $2.00 \% \text{ v/v}$ acetic acid $\text{pH} = 3.00$ with or without chitosan at different concentrations.

To prepare DSPG monolayers at the air –water interface, $30 \mu\text{L}$ of DSPG solution in 1:2 methanol: choloform (0.40mg/mL) was carefully spread at the surface with a Hamilton micro-syringe. Before spreading DSPG solution, the subphase surface was cleaned by sweeping it with the Teflon barriers and then, any surface contaminant was removed by

suction from the interface. The cleaning of the surface was checked by recording an isotherm in absence of DSPG and verifying a surface pressure value lower than 0.20 mN/m. After spreading, the solvent was allowed to evaporate during 10 min, and then the film was compressed with two barriers, one on each side of the trough at a compression speed of 5 mm/min while the automatic measurement of the lateral surface pressure (π) was carried out.

All experiments were performed at 25 ± 1 °C using a HAAKE G. thermostat. At least two compression isotherms were registered at each condition and results with a typical area and collapse pressure errors of ± 2 Å² and ± 1 mN.m⁻¹ respectively were obtained.

The surface compression modulus κ (mN.m⁻¹) was calculated from the compression isotherm as:

$$\kappa = -A \times \left(\frac{\partial \pi}{\partial A} \right)_T \quad (1)$$

where A is the molecular area per molecule and π is the surface pressure in mN.m⁻¹. The uncertainty of compression modulus was ± 10 mN. m⁻¹.

2.4.2 Surface potential - molecular area isotherms

The Surface potential – molecular area isotherms were measured with a home-made Langmuir balance using an air-ionizing ²⁴¹Am plate surface electrode and an Ag/AgCl/Cl⁻ (3M) reference electrode⁴³.

The composition of the subphases used in these compression isotherms were the same as in section 2.4.1.

To prepare DSPG film monolayer at the air-water interface volumes between 15-25 µL of DSPG in 1:2 methanol: chloroform solution (0.40mg/mL) were carefully spread at the

surface with a Hamilton micro-syringe. The experiments were performed after 10 min of the injection. The film was compressed with one barrier at a compression speed of 13 mm/min. Lateral pressure was registered simultaneously and the lateral pressure-molecular area isotherms obtained with this equipment were similar to the obtained as explained in Section 2.4.1.

2.5. Brewster Angle Microscopy (BAM)

The BAM experiments were carried out using an EP3 Imaging ellipsometer (Acucurion, Goettingen, Germany) with a 20x or a 10x objective. The monolayer was formed in a Langmuir film balance (KSV minitrough, KSV Instruments, Ltd., Helsinki, Finland) using the same volumes and DSPG solution than those described in section 2.4.1. Images were registered after 10 min from the injection of DSPG solution, in simultaneous with the surface pressure-molecular area isotherm.

The optical thickness (h) was calculated from the BAM images taken after the BAM equipment was calibrated. The grey level of each section of the micrograph can then be converted to reflected light intensity (R_p), and h was calculated assuming a smooth but thin interface in which the refractive index varies along the normal to the interface on a distance h , much smaller than the incident light wavelength λ ($\lambda=532\text{nm}$)⁴³, which leads to:

$$h = \frac{\sqrt{R_p}}{\sin(2\theta_B - 90)} \left(\frac{\pi \sqrt{n_1^2 + n_2^2} (n_1^2 - n^2)(n_2^2 - n^2)}{\lambda (n_1^2 - n_2^2) n^2} \right)^{-1} \quad (2)$$

In Equation (2) n_1 , n and n_2 are the air, film and subphase refractive index, respectively and θ_B is the Brewster angle.

The refractive index used for DSPG monolayers in the absence of chitosan was 1.45, since this is the value reported for condensed films⁴⁴. As detailed below, when chitosan was present in the subphase the DSPG film became more expanded and then, the refractive index is expected to decrease⁴⁵. Since the refractive index at this condition was unknown, we determined the monolayer thicknesses using 1.42 (index for liquid expanded phases) and 1.45 (index for liquid condensed phases)⁴⁵ and in this way could evaluate the whole range of possible height values. The refractive index for the subphases was calculated for each experiment from the experimental Brewster angle ($n_2 = tg(\theta_b)$), using 1.00 as the refractive index of air) obtaining the following values: 1.336 for the subphase with MCl_z ($M = Li^+$ or Ca^{2+}) $1.00 \times 10^{-2} M$ - 2.00 % v/v acetic acid in absence and 1.337 in presence of chitosan.

3. Results and Discussion

3.1 Cyclic Voltammetry

The effect of chitosan on DSPG monolayers was analyzed by cyclic voltammetry adding the polymer to the aqueous phase before or after the film formation at the water/1,2-dichloroethane interface. The results obtained are shown below in sections 3.1.1. and 3.1.2. The comparison of these results allows evaluating if chitosan modifies the adsorption of DSPG molecules or the structure of the film previously adsorbed.

3.1.1 Effect of chitosan on DSPG adsorption

Figure 1a shows the voltammetric response corresponding to TEA^+ transfer across the bare interface (solid line) and in the presence of DSPG monolayer formed after 60 min of injecting 50 μL of 1mM DSPG solution onto aqueous phases containing LiCl as supporting electrolyte and chitosan in a concentration range from 0 to 1.00 % w/v. Solid line corresponds to the very well known reversible diffusion controlled behavior of TEA^+ transfer process across the bare liquid – liquid interface. A forward current peak at $E_p = 0.480 \text{ V}$ and the corresponding backward process with a peak to peak separation $\Delta E_p = 0.060 \text{ V}$ can be observed. The peak current, I_p , is linear with $v^{1/2}$ over the whole range of sweep rates analyzed (not shown). If this response is compared with that obtained when the DSPG molecules are present at the interface, in absence of chitosan in the aqueous phase, an important decrease in current and a shift of 0.200 V for the positive peak potential towards more positive values and 0.120 V for the negative peak potential towards more negative values can be noticed. These changes are evidencing a blocking effect of the layer to TEA^+ transfer since it can be assumed that the transfer potential shift is due to the increase in Gibbs energy on transfer caused by the work of permeation of species across the film. However this effect decreases as chitosan concentration in aqueous phase increases, almost disappearing for a concentration equal to 1.00 % w/v and recovering a voltammetric response close to the original one. This is a demonstration that chitosan produces disorder on the film or formation of bare zones (pores), minimizing its blocking effect on TEA^+ transfer.

Figure 1b summarizes the effect of chitosan concentration on the DSPG monolayer structure. The variation of current values at $E_p = 0.480 \text{ V}$ is plotted vs chitosan concentration

1
2
3 in absence (\blacktriangle) and in presence (\bigcirc) of the monolayer. The decrease in current values in
4
5 absence of the film can be explained considering a decrease in diffusion coefficient of TEA^+
6
7 caused by the increase in viscosity of the aqueous phase with the chitosan concentration as it
8
9 will be demonstrated below. When the monolayer is present, a marked decrease in current is
10
11 observed in absence of chitosan in aqueous phase, nevertheless, for chitosan concentrations
12
13 within the range 0.02 – 0.15 % w/v, it sharply increases from almost zero to values close to
14
15 that observed in absence of the film. For chitosan concentration values higher than 0.20 %
16
17 w/v a slight decrease followed by constancy in current values are reached as a consequence of
18
19 the decrease in diffusion coefficients already noted in absence of the film.
20
21
22
23

24 A significantly different response is obtained when LiCl is replaced by CaCl_2 as
25
26 aqueous supporting electrolyte as can be observed in Figure 2. It is evident from these results
27
28 that the blocking effect to TEA^+ transfer caused by the monolayer is not reversed by the
29
30 presence of chitosan even at high concentration values. These different voltammetric
31
32 responses depending on the cation present in aqueous phase can be explained taking into
33
34 account that Ca^{2+} cations produce an important structuring effect on DSPG monolayers due to
35
36 their strong interaction with the partially ionized anionic polar head groups of phospholipids
37
38 which diminish the lateral electrostatic repulsions as it has already been reported⁴⁶. Under
39
40 these conditions, chitosan is not able of disorganizing the film, probably due to the
41
42 impediment to penetrate into these very tightly compacted monolayers.
43
44
45
46
47

48 Summing up, the results obtained up here indicate that DSPG monolayer has a
49
50 blocking effect on TEA^+ transfer, but its structure and permeability depend on the cation
51
52 present in water, obtaining the highest ordered films in the case of Ca^{2+} . When chitosan is
53
54 present in aqueous phase it is able to incorporate into DSPG monolayers formed in the
55
56
57
58
59
60

presence of Li^+ producing disorganization on them, nevertheless this effect is not observed for the highly structured films formed in presence of Ca^{2+} .

3.1.2 Effect of chitosan on DSPG films previously formed

In this series of experiments the DSPG monolayer was first generated at the interface air / gelled organic phase, as described in experimental section, and subsequently this organic phase, containing the monolayer, was put in contact with the aqueous phase containing LiCl or CaCl_2 as supporting electrolyte in absence or in presence of chitosan. The voltammetric results are shown in Figure 3a and 3b. As it can be noted, similar responses to those in Figures 1a and 2 for LiCl and CaCl_2 , respectively, are obtained. In the same way, the insets in these figures indicate that increasing chitosan concentration leads to increasing current values when LiCl is the aqueous electrolyte, however no changes in current values are observed in the case of CaCl_2 .

From the comparison of the results informed in sections 3.1.1 and 3.1.2 it can be concluded that chitosan produces disordering or pores on DSPG monolayers previously formed and also this polymer modifies the adsorption of DSPG molecules at the water/1,2-DCE interface, provided LiCl is the aqueous electrolyte.

Finally, Figure 4 summarizes the effect of chitosan in presence of LiCl (\square) or CaCl_2 (\bullet). For this purpose a blocking ratio for each chitosan concentration value was calculated as:

$$\left(\frac{I_{chi}^{TEA^+} - I_{chi}^{TEA^+, DSPG}}{I_{chi}^{TEA^+}} \cdot 100 \right) \quad (3)$$

where $I_{chi}^{TEA^+}$ and $I_{chi}^{TEA^+,DSPG}$ are the peak current values for TEA^+ transfer process for each chitosan concentration in absence or in presence of DSPG monolayer respectively. As it can be noted, the blocking effect of the monolayer sharply decreases from 100 % to values close to 0 % as chitosan concentration increases in the case of LiCl, while it remains constant at values close to 100% when $CaCl_2$ is the aqueous electrolyte.

3.2 Viscosity Experiments

As it was discussed above in Figure 1b, section 3.1.1, the transfer of TEA^+ from the aqueous to the organic phase is modified when chitosan is present in the aqueous solution even in absence of DSPG. It was noted in Figure 1b (black triangle) that as chitosan concentration increases, the TEA^+ transfer current decreases. This behavior could be explaining considering that high concentrations of chitosan produce an increase in the viscosity of the aqueous phase and, as consequence, the diffusion rate of TEA^+ from the bulk of the aqueous solution to the interface decreases. To corroborate this hypothesis, viscosity measurements were performed at $(25 \pm 1)^\circ C$ and the diffusion coefficients of TEA^+ at different chitosan concentration were calculated.

The viscosity measurements of chitosan solutions were made as described in section 2.3. From these experiments, flow curves or rheogram, plots of shear stress (τ/Pa) versus shear rate ($\dot{\gamma}/s^{-1}$), for different chitosan solutions were obtained and are shown in Figure 5. As can be seen, all the solutions studied (chitosan in a concentration range from 0 to 1.00 % w/v) present a linear flow behavior, which is characteristic of a Newtonian fluid⁴⁷, whose regimen obeys the following equation:

$$\tau = \dot{\gamma} \eta \quad (4)$$

where η is the apparent viscosity of the solution. According to this equation, the apparent viscosities for chitosan solutions were determined from the slope of the plots in Figure 5 (Table 1). As it was expected the viscosity of chitosan solutions increase with the concentration.

On the other hand, the diffusion coefficients of TEA^+ in aqueous phase were calculated for all the chitosan solutions studied. The relation between the diffusion coefficient of TEA^+ and the peak current of transfer is given by the equation:

$$I_p^{\text{TEA}^+} = 0,4463 \cdot z \cdot F \cdot A \cdot c^{\text{TEA}^+} \cdot D_{\text{TEA}^+}^{1/2} \left(\frac{z \cdot F \cdot v}{R \cdot T} \right)^{1/2} \quad (5)$$

where, $I_p^{\text{TEA}^+}$ is the peak current for TEA^+ transfer at each chitosan concentration; z is the charge of TEA^+ ; F the Faraday constant; A the interfacial area (0.16 cm^2); c is the concentration of TEA^+ in aqueous phase ($5.00 \times 10^{-4} \text{ M}$); D is the diffusion coefficient of TEA^+ , v is the sweep rate (0.05 V.s^{-1}), R the gases constant and T the temperature at witch the experiments were performed⁴⁸. The resulting D values are also listed in Table 1 and, as it can be noted, they decrease when chitosan concentration increases.

Figure 6 shows the dependence of diffusion coefficient of TEA^+ with the inverse of the solution viscosity (η^{-1}). From this graphic it is evident that there is a linear relationship between both parameters, with a correlation coefficient of 0.9644 and random residues (inset Figure 6). The linear relationship can be described in function of the Stoke-Einstein relation:

$$D = \frac{k_b \cdot T}{f} \quad (6)$$

where: k_b is the Boltzman constant; f is the frictional coefficient, a measure of the force retarding a molecule's motion. For a spherical particle of radius a in a solvent of viscosity η ,

the frictional coefficient is given by $f = 6\pi a \eta$ ^{49, 50}. So that, from the slope of Figure 6, and assuming a spherical geometry for TEA⁺, a radius $a = 6.0 \text{ \AA}$ could be calculated. The radius of the TEA⁺ cation, without any associated water molecules, has been reported as 3.4 \AA in a theoretical work on the Gibbs energies of ion transfer at ITIES⁵¹. The greater value obtained from the present experimental results can be due to the hydration sphere of TEA⁺ in solution, not considered in the theoretical calculation.

These results confirm that the increasing concentration of chitosan in aqueous phase produces a diminution in diffusion coefficient of TEA⁺, explaining the decrease in peak currents pointed out in section 3.1.1.

3.3 *Langmuir Monolayers*

3.3.1 *Surface Pressure-molecular area isotherms*

The effect of chitosan on the partially ionized anionic DSPG monolayer can be noted in Figure 7. This figure shows the surface pressure-area isotherm obtained at 25°C in absence and in presence of different chitosan concentrations using LiCl (Figure 7a) and CaCl₂ (Figure 7b) in the subphase. The isotherms obtained in absence of chitosan (solid line) in both media show a change of slope characteristic of the gaseous-liquid condense phase transition. The DSPG monolayer collapse is evident at surface pressures of 48 mN.m^{-1} , with mean molecular areas of 35 \AA^2 and 38 \AA^2 for LiCl and CaCl₂ subphases respectively. Important changes in the surface pressure -area isotherms are visible when DSPG monolayer is spread on the subphases containing chitosan in both media. As it can be noted in the Figure 7 the isotherms shift towards larger areas per molecule, indicating that chitosan was incorporated to the film at low

pressures, and this is an evidence that chitosan produce an expansion of the DSPG film^{25, 52, 53}. This expansion can also be deduced from the compression modulus values, κ (mN.m⁻¹), which allow classifying the state of the monolayer as: liquid-expanded (κ =10-100 mN.m⁻¹), liquid-condensed (κ =100-250 mN.m⁻¹) and condense (κ > 250 mN.m⁻¹)⁵⁴. Table 2 shows the values of κ obtained at a constant pressure equal to 40 mN.m⁻¹ and, as it can be observed, the results indicate that in absence of chitosan the state of the monolayer corresponds to liquid – condensed phase for either, LiCl or CaCl₂ subphases. Nevertheless, as chitosan concentration increases, the modulus κ decreases reaching values of 25-30 mN.m⁻¹ for the highest chitosan concentration employed. This observation indicates the presence of a new component at the interface, which produces changes in the state of the monolayer from liquid-condense to liquid-expanded phase. The great change of the compression modulus at high surface pressures was attributed, by J. Paviatto et.al., to the interaction between chitosan and the phospholipid polar head group which makes the film more flexible⁵³. This effect can be clearly observed in Figure 8a where the change in the area per molecule ($\Delta A = A^{\text{in presence of chitosan}} - A^{\text{in absence of chitosan}}$), produced by chitosan, at 25 mN.m⁻¹ and 40 mN.m⁻¹ are shown. As can be noted, the increase in area is more pronounced at low pressure, condition at which the incorporation of chitosan into the film is more feasible. As the monolayer is compressed (pressure 40 mN.m⁻¹), lower values of ΔA are obtained, as a consequence of the expelling of a certain amount of chitosan from the surface. On the other hand, comparing ΔA values for subphases containing LiCl or CaCl₂, it is evident that in the first case the shift of the isotherm, towards higher A values, is more important. An explanation for this behavior can be found in the higher charge density of Ca²⁺ compared with Li⁺, which leads to a higher accumulation of this cation at the surface where the negative charge of polar head groups of DSPG are located, and, additionally, to a direct binding to the phosphate groups of DSPG. The strong interaction

1
2
3 Ca^{2+} - phosphate results in the reduction of the electrostatic repulsion between the polar head
4 groups and an enhancement of the interaction between the hydrocarbon tails of DSPG leading
5 to a greater structuring of the monolayer. The effect on monolayer condensation produced by
6 different cations has been also shown by means of electrochemical experiments for various
7 phospholipid^{33,37,39}. Based on these reports and considering the results shown in Figure 8, it
8 can be stated that chitosan may be incorporated in the monolayer in a more effective way
9 when LiCl is present in the subphase instead of CaCl_2 , producing an important change in the
10 resulting average molecular area.
11
12
13
14
15
16
17
18
19
20
21

22 The effect of expansion of the DSPG film produced by chitosan is also evident when
23 the pressure and the molecular area in the collapse, as a function of chitosan concentration,
24 are analyzed. Figure 8b shows this variation for subphases containing LiCl (circles) or CaCl_2
25 (squares). For both cases an enhancement of the collapse molecular area with the increasing
26 chitosan concentration was observed. This result demonstrates that chitosan is not completely
27 expelled from the interface when the monolayer arrive to the collapse, at this point chitosan
28 remains in the interface interacting with the partially ionized negative polar head groups of
29 DSPG. It can also be observed in Figure 8b that DSPG monolayers in the presence of chitosan
30 collapse at surface pressures lower than those of pure DSPG, thus indicating that they are less
31 stable than the pure monolayer.
32
33
34
35
36
37
38
39
40
41
42
43
44

45 Furthermore, hysteresis studies has been carried out for pure DSPG and mixed
46 chitosan-DSPG monolayers, Figure 9. For pure DPPG monolayer non hysteresis is observed
47 (grey line) in the isotherm. On the opposite, for chitosan-DSPG monolayers a significant
48 hysteresis is observed (black line), probably due to the formation of an irreversible complex
49 between DSPG and chitosan which can aggregate at the interface. This effect has been
50
51
52
53
54
55
56
57
58
59
60

previously reported by Pavinatto et. al. for DPPG and DPPC monolayers in the presence of chitosan⁵³.

3.3.2 Surface Potential-area isotherms

Figure 10a shows the change of surface potential per molecular area ($\Delta V.A$) as function of the mean molecular areas, for DSPG monolayer at different chitosan concentration in the subphase. As the monolayer is compressed, the surface potential increases as a consequence of the orientation of polar head groups, the hydrocarbon chains or the hydration water at the interface. When chitosan is present, an excess of positive charge is present at the interface interacting with the polar head groups of DSPG generating an alteration of the average vertical component of the dipole moment of DSPG molecules and producing an enhancement of surface potential. Another explanation for this increase in potential can be found in the reorganization of the dipolar moment of the interfacial molecules of water around chitosan²⁶. Similar effect was observed when the subphase contained CaCl_2 as electrolyte (data not shown).

Figure 10b shows the change of surface potential per unit of area produced by different chitosan concentration, calculated as: $(\Delta (\Delta V.A)) = (\Delta V.A_{\text{with chit}} - \Delta V.A_{\text{without chit}})$ at two lateral pressures (25 and 40 mN.m^{-1}), as a function of the chitosan concentration in subphases containing LiCl (circles) or CaCl_2 (squares). As can be observed, the increase of surface potential is evident for LiCl subphases both at low (25 mN.m^{-1}) and high pressures (40 mN.m^{-1}), indicating that chitosan prevails interacting with the phospholipid and is not expelled from the interface to the bulk subphase, even at pressures near to the collapse. Nevertheless, chitosan generates higher increases of the surface potential when the film is at

low pressure, corresponding with the fact that chitosan can penetrate more efficiently in the DSPG film contributing with its positive charge. When the subphase contains CaCl_2 almost constant Δ ($\Delta V.A$) values are observed over the whole range of chitosan concentrations at high pressure, while comparing the response obtained for LiCl and CaCl_2 at low pressure, it is evident that the increase in Δ ($\Delta V.A$) is more pronounced when LiCl is present in the subphase. This is in agreement with the fact that the films generated in presence of LiCl are less condensed than those formed in presence of CaCl_2 , as discussed above in section 3.3.1, allowing a better incorporation of chitosan into the DSPG monolayer.

3.4 Brewster Angle Microscopy (BAM)

Brewster angle microscopy studies were performed with the aim of confirming the presence of chitosan at the interface interacting with the DSPG monolayer. Figure 11a shows representative micrographs obtained by BAM, for the DSPG film in absence (i) and in the presence (ii) of 0.06 % w/v solution of chitosan in 1×10^{-2} M CaCl_2 and 2.00 % v/v acetic acid, at different lateral pressures. As it can be observed, there is a noticeable difference between the gray levels of the micrograph for DSPG films and mixed DSPG-chitosan films. As stated in the previous sections, we attribute these differences to the fact that chitosan interacts with DSPG molecules, both at low and high pressures, generating an enhancement in the surface thickness. The difference in gray levels was also observed using LiCl as aqueous electrolyte (micrograph not shown).

With the purpose of showing the results in a more quantitative manner, the optical thickness of the monolayer was calculated using the Equation (2). The refractive index used for DSPG monolayers in the absence of chitosan was 1.45, since this is the value reported for

condensed films⁴⁴. When chitosan is present in the subphase the DSPG film becomes less dense and then, the refractive index is expected to decrease⁴⁵. Since the refractive index at this condition was unknown, we determined the optical thicknesses of the monolayer using 1.42 (refractive index for a liquid expanded phases) or 1.45⁴⁴ (refractive index for a liquid condensed phases) and the whole range of possible optical thicknesses values as function of surface pressure were plotted in Figures 11 b and c in comparison with values obtained in absence of chitosan.

For both electrolytes (LiCl or CaCl₂) the monolayer thickness in absence of chitosan was around 20 Å. When chitosan is present in the subphase, the thickness values are in the range between 30 and 50 Å, overcoming the values obtained for pure DSPG monolayer for all the pressure measured. These results are another evidence that chitosan is present at the interface, interacting with DSPG molecules, even at high lateral pressure values.

4. Conclusions

Taking into account the results obtained in the present paper, we propose the model shown in scheme 2 for the interaction between DSPG and chitosan. In this model two stages for the interaction of chitosan with DSPG can be distinguish: (a) in first place, at low pressures (large molecular areas), the interaction is driven by Van der Waals forces between the DSPG hydrocarbon tails and the hydrophobic zones of chitosan. This interaction is facilitated by chitosan penetration into the monolayer in gaseous state. Beside the hydrophobic interaction, electrostatic attraction between the phosphate groups of DSPG and the positive charged amino groups of chitosan can also be established (Scheme 2.a).

(b) Secondly, at high pressures, chitosan is partially expelled from the interface, but it remains at the interface interacting with DSPG monolayer probably through electrostatic interaction between phosphate and the amino groups.

The situation at liquid / liquid interfaces with LiCl as aqueous electrolyte is, probably, similar to that shown in scheme 2a, obtaining a blocking film in absence of chitosan and a more permeable one in presence of the polymer, explaining in this way the electrochemical results. On the other hand, the presence of CaCl_2 as supporting aqueous electrolyte produces more compact monolayers, similar to that shown in scheme 2b, which can not be penetrated by chitosan molecules prevailing the blocking effect of DSPG film to TEA^+ transfer.

5. Acknowledgements

Financial support from Consejo Nacional de Investigaciones Científicas y Tecnológicas (CONICET), Agencia Nacional de Promoción Científica y Tecnológica (FONCyT) and Secretaría de Ciencia y Técnica de la Universidad Nacional de Córdoba (SECyT) is gratefully acknowledged. C.I. Cámara and M.V. Colqui Quiroga wish to thank CONICET for the fellowships awarded. A. Jimenez – Kairuz, N. Wilke and L.M. Yudi are members of the Research Career of CONICET.

6. References

- [1] Sui, W.; Song, G.; Chen, G.; and Xu, G. *Colloid Surf. A: Physichchem. Eng. Aspects*. **2005**, 356, 29-33.
- [2] Rinaudo, M.; *Prog. Polym. Sci.* **2006**, 31, 603-620
- [3] Tharanathan, R. N.; Kittur, F. S.; *Crit. Rev. Food Sci. Nutr.* **2003**, 43, 61-87
- [4] Ravi Kumar M.N.V.; *Reactive and Functional Polym.* **2000**, 46, 1-27.
- [5] M. Yalpani, F. Johnson, L.E. Robinson. Chitin, Chitosan: Sources, Chemistry, Biochemistry, *Physical Properties and Application*, Elsevier, Amsterdam, **1992**.
- [6] Ausar, S. F.; Bianco, I. D.; Badini, R. G.; Castagna, L. F.; Modesti, N. N.; Landa, C. A.; Beltramo, D. M. *J. Dairy Sci.*, **2001**, 84, 361-369.
- [7] Wu, F. C.; Tseng R. L.; Juang, R.S. *J. Environ. Manag.* **2010**, 91, 798-806.
- [8] Krajawska, B.; *Sep. Purif. Technol.* **2005**, 41, 305-312.
- [9] Shields, K. M.; Smock, N.; McQueen, C. E.; Bryant, P. J.; *Am. J. Helth-Syst. Pharm.* **2003**, 60, 1310-1312.
- [10] Sun, J.; Jiang, G.; Wang, Y.; Ding, F. *J. Appl. Polym. Sci.* **2012**, 125, 2092-2101.
- [11] Yun-Huan J.; Hai-Yang H.; Ming-Xi Q.; Jia Z.; Jia-Wei Q.; Chan-Juan H.; Qiang Z.; Da-Wei C. *Colloid and Surfaces B: Biointerface.* **2012**, 94, 184-191.
- [12] Kima, T.-H.; Jianga, H.-L.; Jerea, D.; Parka, I.-K.; Chob, M.-H.; Nahc, J.-W.; Choia, Y.-J.; Akaiked, T.; Choa, C.-S. *Prog. Polym. Sci.* **2003**, 48, 358-365.
- [13] Shahidi, F.; Vidana Arachchi, J. K.; Jean, Y-J. *Trends in Food Science & Technology.* **1999**, 10, 37-51.
- [14] Okamoto, Y.; Yano, R.; Miyatake, K.; Tomohiro, I.; Shigemasa, Y.; Minami, S. *Carbohydr. Polym.* **2003**, 53, 337-342.

- [15] Fang, N. and Chan, V. *Biomacromolecules*. **2003**, 4, 581-588.
- [16] Caseli, L.; Pavinatto, F. J.; Nobre, T. M.; Zaniquelli, M. E. D.; Viitala, T.; Oliveira, O. N. Jr. *Langmuir*. **2008**, 24, 4150-4156.
- [17] Silva, C. A.; Nobre, T. M.; Pavinatto, F. J.; Oliveira, O. N. Jr. *J Colloid and Interface Sci*. **2012**, 376, 289-295.
- [18] Campiña, J. M.; Souza, H. K. S.; Borges, J.; Martins, A.; Gonçalves, M. P.; Silva, F. *Electroch. Acta*. **2010**, 55, 8779-8790.
- [19] Krajewska, B.; Wydro, P.; Janczyk, A. *Biomacromolecules*. **2011**, 12, 4144-4152.
- [20] Pavinatto, F. J.; Pacholatti, C. P.; Montanha, E. A.; Caseli, L.; Silva, H. S.; Miranda, P. B.; T., Oliveira, O. N. Jr. *Langmuir*. **2009**, 25, 10051-10061.
- [21] Fang, N. and Chan, V. *Biomacromolecules*. **2003**, 4, 1596-1604.
- [22] Yang, F.; Cui, X.; Yang, Xiurong. *Biophysica Chemistry*. **2002**, 99, 99-106.
- [23] Chan, V.; Mao, H.-Q.; Leong, K. M. *Langmuir*. **2001**, 17, 3749-3756.
- [24] Fang, N.; Chan, V.; Mao, H.-Q.; Leong, K. M. *Biomacromolecules*. **2001**, 2, 1161-1168.
- [25] Parra-Barraza, H.; Burboa, M.G.; Sánchez-Vazquez, M.; Juárez, J.; Goycoolea, F. M. G.; Valdez, M. A.; *Biomacromolecules*. **2005**, 6, 2416-2426.
- [26] Pavinatto, F. J.; Caseli, L.; Pavinatto, A.; dos Santos, D. S. Jr.; Nobre, T. M.; Zaniquelli, M. E. D.; Silva, H. S.; Miranda, P. B.; T., Oliveira, O. N. Jr. *Langmuir*. **2007**, 23, 7666-7671.
- [27] Silva, C. A.; Nobre, T. M.; Pavinatto, F. J.; Oliveira, O. N. Jr. *J Colloid and Interface Sci*. **2012**, 376, 289-295.
- [28] Roozeman, R. J.; Liljeroth, P.; Johans, C.; Williams, D. E.; Kontturi, K. *Langmuir*. **2002**, 18, 8318-8323.

- [29] Marecek, V.; Lhotsky', A.; Jänchenová, H. *J. Phys. Chem. B.* **2003**, 107, 4573-4578.
- [30] Jänchenová, H.; Stulik, K.; Marecek, V. *J. Electroanal. Chem.* **2007**, 601, 101-106.
- [31] Ivlehan, F.; Lanyon, Y. H.; Arrigan, D. W. M. *Langmuir.* **2008**, 24, 9876-9882.
- [32] Georganopoulou, D. G.; Strutwolf, J.; Pereira, C. M.; Silva, F.; Unwin, P. R.; Williams, D. E. *Langmuir.* **2001**, 17, 8348-8354.
- [33] Berduque, A.; Scanlon, M. D.; Collins, C. J.; Arrigan, D. W. M. *Langmuir.* **2007**, 23, 7356-7364.
- [34] Chesniuk, S. G.; Dassie, S. A.; Yudi, L. M.; Baruzzi, A. M. *Electrochim. Acta.* **1998**, 43, 2175-2181.
- [35] Maeda, K.; Yoshida, Y.; Goto, T.; Marecek, V. *J. Electroanal. Chem.* **2004**, 567, 317-323.
- [36] Mendez, M. A.; Prudent, M.; Su, B.; Girault, H. H. *Anal. Chem.* **2008**, 80, 9499-9507.
- [37] Jänchenová, H.; Stulik, K.; Marecek, V. *J. Electroanal. Chem.* **2007**, 604, 109-114.
- [38] Monzón, L. M. A.; Yudi, L. M. *Electrochim. Acta.* 2006, 51, 1932-1940.
- [39] Monzón, L. M. A.; Yudi, L. M. *Electrochim. Acta.* 2006, 51, 4573-4581.
- [40] Monzón, L. M. A.; Yudi, L. M. *Electrochim. Acta.* **2007**, 52, 6873-6879.
- [41] Colqui Quiroga, M. V.; Monzón, L. M. A.; Yudi, L. M. *Electrochimica Acta.* **2011**, 56, 7022-7028.
- [42] Colqui Quiroga, M. V.; Monzón, L. M. A.; Yudi, L. M. *Electrochimica Acta.* **2010**, 55, 5840-5846.
- [43] Vega Mercado, F.; Maggio, B.; Wilke, N. *Chemestry and Physics of Lipids.* **2011**, 164, 386-392.
- [44] Petrov, J. G.; Pfohl, T.; Mohwald, H. *J Phys. Chem. B.* **1999**, 103, 3417-3424.

- [45] Ducharme, D.; Max, J. J.; Salesse, C.; Leblanc, R. M. *J Phys. Chem.* **1990**, *94*, 1925-1932.
- [46] Garidel, P. and Blume, A. *Chemistry and Physics of Lipids.* **2005**, *138*, 50-59.
- [47] J. Desbrieres. *Biomacromolecules.* **2002**, *3*, 342-349.
- [48] *Electrochemical Method, Fundaments and Applications.* Allen J. Bard and Larry R. Faulker. 2th edition. **2001**. Pg: 231.
- [49] *Atkins Physical Chemistry.* Peter Atkins and Julio the Paula. 7th edition. Oxford. pg 741-742.
- [50] Srivastava, R. and Khanna, K. N. *J. Chem. Eng. Data*, **2009**, *54*, 1453-1456.
- [51] Dryfe, R.A.WHolmes, S.M. *J. Electroanal. Chem.,.* **2000**, *483*, 144-149.
- [52] Wydro, P.; Krajewska, B.; Katarazyna, H.-W. *Biomacromolecules.* **2007**, *8*, 2611-2617.
- [53] Pavinatto, F. J.; Pavinatto, A.; Caseli, L.; dos Santos, D. S. Jr.; Nobre, T. M.; Zaniquelli, M. E. D.; Oliveira, O. N. Jr. *Biomacromolecules.* **2007**, *8*, 1633-1640.
- [54] Davies, J.T; Rideal, E.K. *Interfacial Phenomena.* **1963**, Academic Press, New York.

Figure captions:

Scheme 1: Structures of chitosan and DSPG.

Scheme 2: Schematic model for DSPG – chitosan interaction at the air / water interface for (a) high or (b) low molecular areas.

Figure 1: (a) Cyclic voltamograms corresponding to the transfer of TEA^+ through the bare interface (—) or 60 min after the injection of 50 μL of 1 mM DSPG in 1:2 methanol:chloroform solution at different concentrations of chitosan: (—) 0, (—) 0.06, (---) 0.10 and (.....) 1.00 % w/v. (b) Dependence of I_p^+ with chitosan concentration: in presence (\circ) or in absence (\blacktriangle) of DSPG film. Aqueous phase composition: $1 \times 10^{-2} \text{M}$ LiCl, 2.00 % v/v Acetic Acid, $5 \times 10^{-4} \text{M}$ TEA^+ , and different concentrations of chitosan, pH=3.00. Organic phase composition: $1 \times 10^{-2} \text{M}$ TPhAsDCC. $v = 0.050 \text{ V s}^{-1}$.

Figure 2: Cyclic voltamograms corresponding to the transfer of TEA^+ through the bare interface (—) or 60 min after the injection of 50 μL of 1 mM DSPG in 1:2 methanol:chloroform solution at different concentrations of chitosan: (—) 0, (—) 0.02, (---) 0.25 % and (.....) 1.00 % w/v. Aqueous phase composition: $1 \times 10^{-2} \text{M}$ CaCl_2 , 2.00 % v/v Acetic Acid, $5 \times 10^{-4} \text{M}$ TEA^+ , and different concentrations of chitosan, pH=3.00. Organic phase composition: $1 \times 10^{-2} \text{M}$ TPhAsDCC. $v = 0.050 \text{ V s}^{-1}$.

Figure 3: Cyclic voltamograms for TEA⁺ transfer in absence (—) or in presence of DSPG film previously generated at the interface air / gelled organic phase by the injection of 20μL of DSPG solution. Successive voltammograms were obtained after standard addition of different volumes of 1.00 % w/v chitosan solution in the presence of DSPG film. Final chitosan concentrations (—) 0, (---) 0.01, (---) 0.02, (---) 0.05, (—) 0.06, (.....) 0.10, (— . .) 0.15, (.....) 0.20 and (— —) 0.50 % w/v. Aqueous phase composition: (a) 1x10⁻²M LiCl, 2.00 % v/v Acetic Acid, 5x10⁻⁴ M TEA⁺ (b) 1x10⁻²M CaCl₂, 2.00 % v/v Acetic Acid, 1x10⁻⁴ M. TEA⁺. pH=3.00. Organic phase composition: 2.00mL of 1x10⁻²M TPhAsDCC in DCE, 0.30g PVC (HMW), 30μL of dioctyl sebacate. Aqueous and Organic phases were put in contact after DSPG film formation. $v = 0.050$ Vs⁻¹. Inset: Dependence of Ip⁺ with chitosan concentration in presence of DSPG.

Figure 4: Plot of blocking ratio ($\frac{I_{chi}^{TEA^+} - I_{chi}^{TEA^+, DSPG}}{I_{chi}^{TEA^+}} \cdot 100$) vs chitosan concentration for (□) LiCl or (●) CaCl₂. Organic and aqueous phase compositions are the same than in figure 1 (a) (□) or 2 (●).

Figure 5: Plot of shear stress (τ) as function of shear rate ($\dot{\gamma}$). Aqueous phase composition: 1x10⁻² M LiCl, 2.00 % v/v acetic acid and (■) 0, (●) 0.07, (▲) 0.15, (◄) 0.25, (◆) 0.50, (♦) 1.00 % w/v chitosan.

Figure 6: Dependence of diffusion coefficient of TEA⁺ as a function of the inverse of solution viscosity (η^{-1}). Inset: Plot of residual value of lineal regression vs the inverse of solution viscosity (η^{-1}).

Figure 7: Surface pressure (π) as function of the mean molecular area for DSPG monolayer at the air-water interface. Subphase composition: 2.00% v/v Acetic acid, chitosan: (—) 0, (— —) 0.01, (.....) 0.02 and (— . —) 0.06 % w/v in (a) 1×10^{-2} M LiCl (b) 1×10^{-2} M CaCl_2 . pH= 3.00.

Figure 8: (a) Change in area per molecule at (■, ●) 25 mNm^{-1} and (□, ○) 40 mNm^{-1} for a Langmuir film of DSPG as function of chitosan concentration.. (b) Collapse pressure (□, ○) and collapse area (■, ●) vs chitosan concentration. Subphase composition: 2.00 % v/v acetic acid and (●, ○) 1×10^{-2} M LiCl or (■, □) 1×10^{-2} M CaCl_2 and different chitosan concentrations. pH = 3.00.

Figure 9: Surface pressure (π) as a function of the mean molecular area for one cycle of compression-decompression of DSPG monolayer for subphases containing: 1×10^{-2} M LiCl and (—) 0 or (—) 0.06 % w/v chitosan.

Figure 10: (a) Isotherms of surface potential per area per molecule ($\Delta V.A$) for subphases containing: 1×10^{-2} M LiCl, 2.00 % v/v acetic acid in absence (—) and in presence of chitosan (— —) 0.01, (.....) 0.02 and (— . —) 0.06 % w/v. (b) Variation of $\Delta(\Delta V.A)$ (see text) with chitosan concentration at different pressures: (■, ●) 25 mN/m and (□, ○) 40 mN/m for subphases containing (●, ○) 1×10^{-2} M LiCl or (■, □) 1×10^{-2} M CaCl_2 .

Figure 11: (a) BAM images for monolayers of DSPG in 1×10^{-2} M CaCl_2 , 2.00 % v/v acetic acid, without (i) and with (ii) 0.06 % w/v chitosan. (b)-(c) Monolayer optical thickness for

1
2
3
4
5
6
7
8
9
10
11
12
13
14
15
16
17
18
19
20
21
22
23
24
25
26
27
28
29
30
31
32
33
34
35
36
37
38
39
40
41
42
43
44
45
46
47
48
49
50
51
52
53
54
55
56
57
58
59
60

subphases containing 2.00% v/v acetic acid and (a) 1×10^{-2} M LiCl or (b) 1×10^{-2} M CaCl_2 in absence (●) and in presence (■) of chitosan (whole range of possible values).

Table 1: Values of apparent viscosity (η) for aqueous solutions with increasing chitosan concentration calculated from the slopes of plots in Fig. 5, and diffusion coefficients for TEA^+ at every chitosan concentration, obtained from voltammetric peak currents.

Table 2: Compression modulus, κ , for DSPG monolayer formed on subphases containing 1×10^{-2} M LiCl or 1×10^{-2} M CaCl_2 in absence or in presence of different chitosan concentrations. The values of κ were calculated at $\pi = 40 \text{ mN.m}^{-1}$.

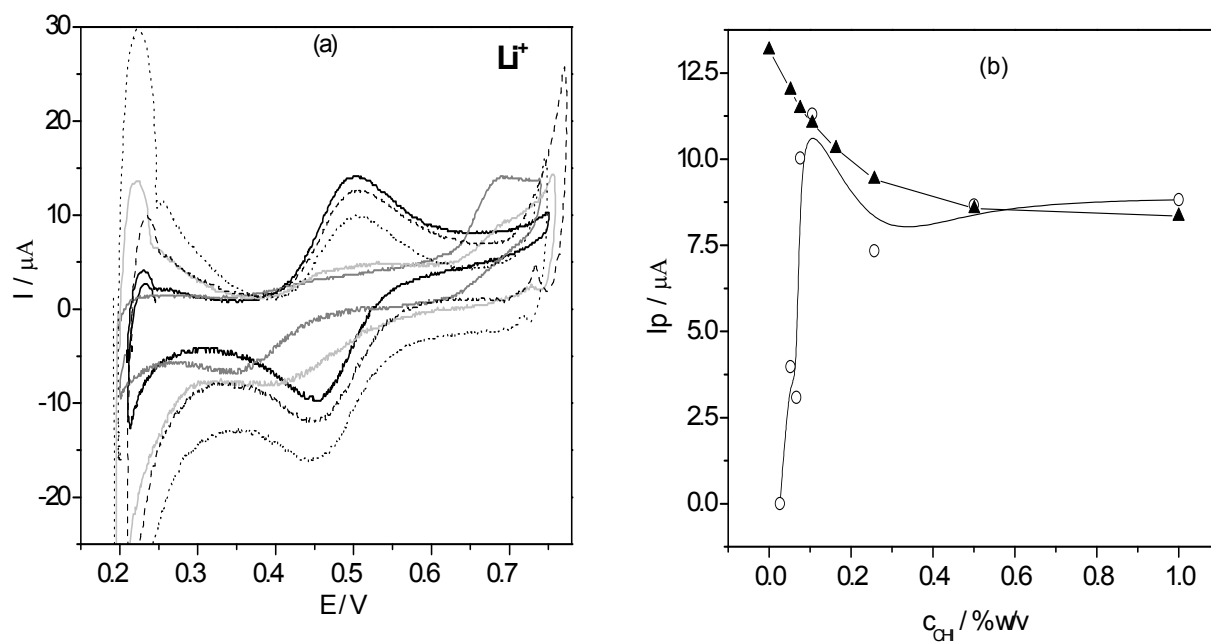


Figure 1: C. I. Cámara, M. V. Colqui, N. Wilke, A. Jimenez-Kairuz and L. M. Yudi.

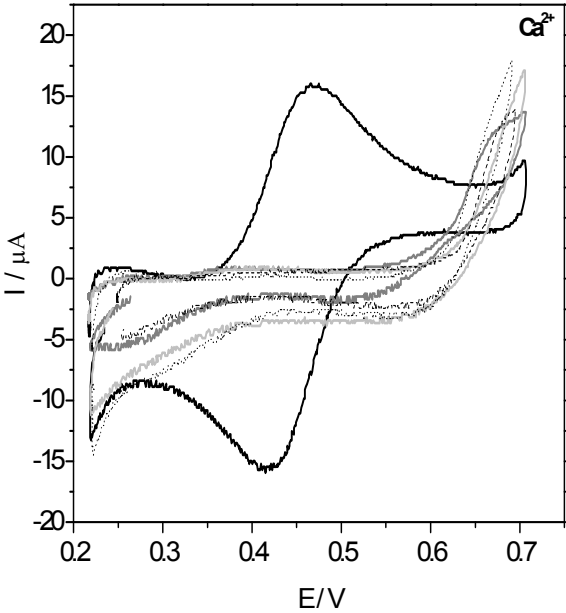


Figure 2: C. I. Cámara, M. V. Colqui, N. Wilke, A. Jimenez-Kairuz and L. M.Yudi.

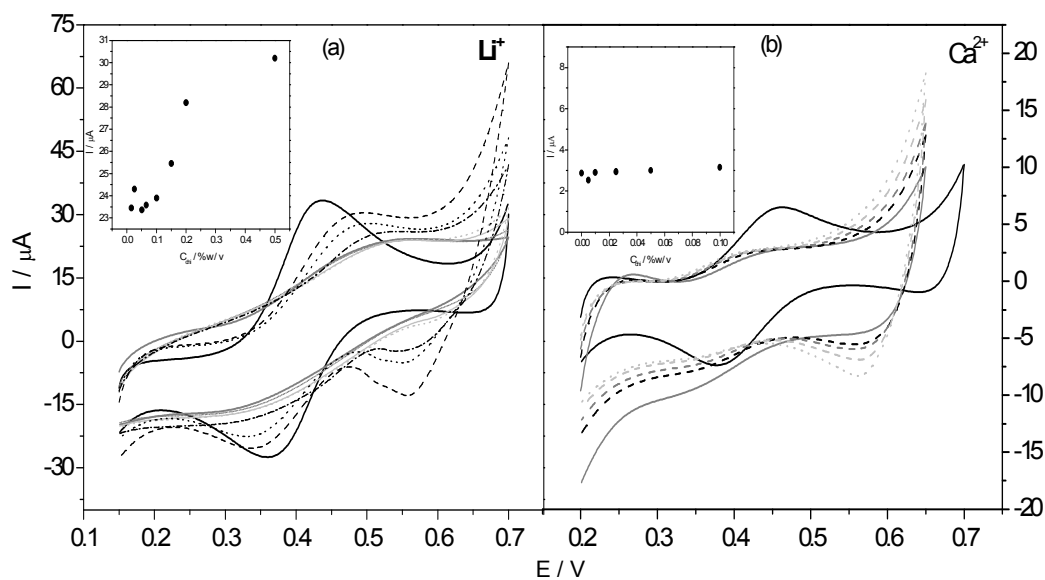


Figure 3: C. I. Cámara, M. V. Colqui, N. Wilke, A. Gimenez Kairus and L. M. Yudi.

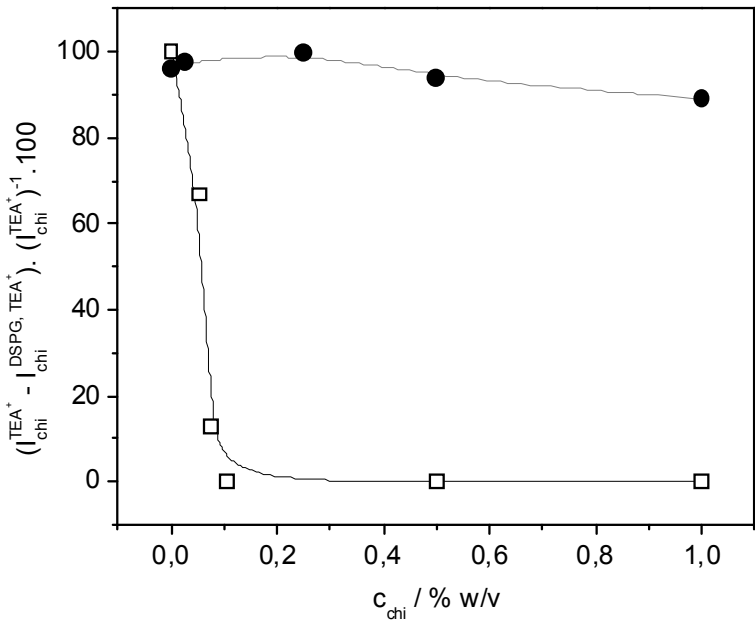


Figure 4: C. I. Cámara, M. V. Colqui, N. Wilke, A. Jimenez-Kairuz and L. M.Yudi.

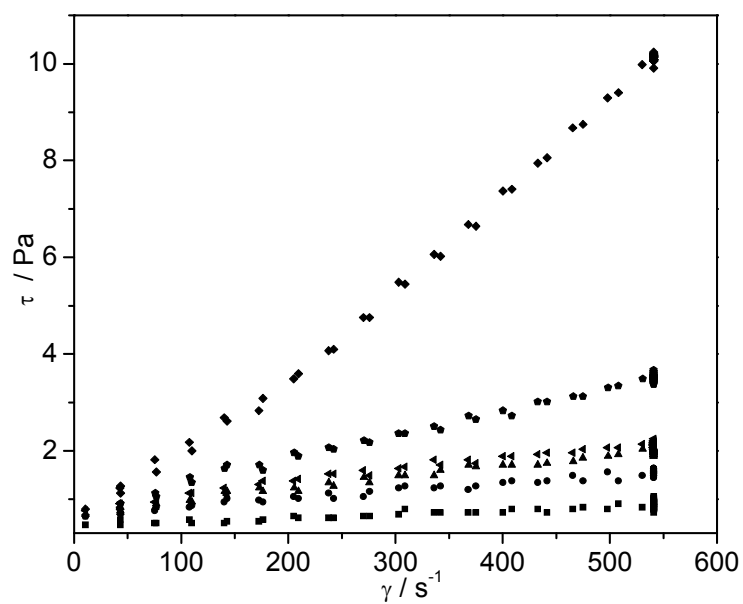


Figure 5: C. I. Cámara, M. V. Colqui, N. Wilke, A. Jimenez-Kairuz and L. M.Yudi.

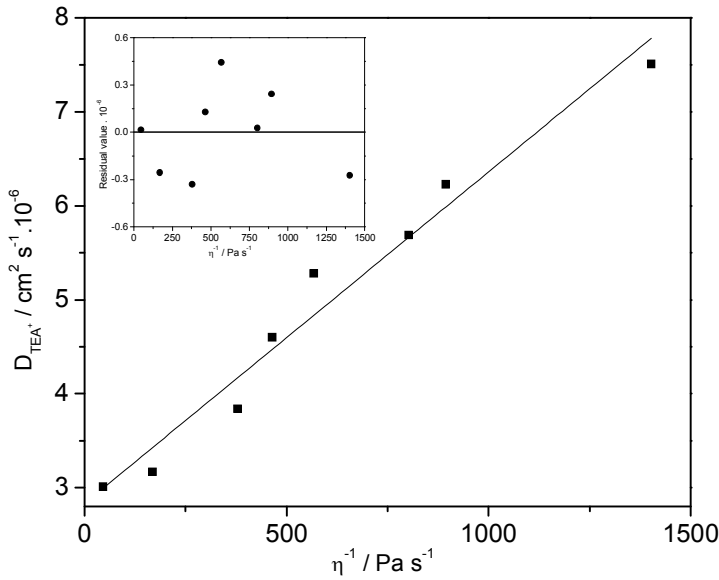


Figure 6: C. I. Cámara, M. V. Colqui, N. Wilke, A. Jimenez-Kairuz and L. M.Yudi.

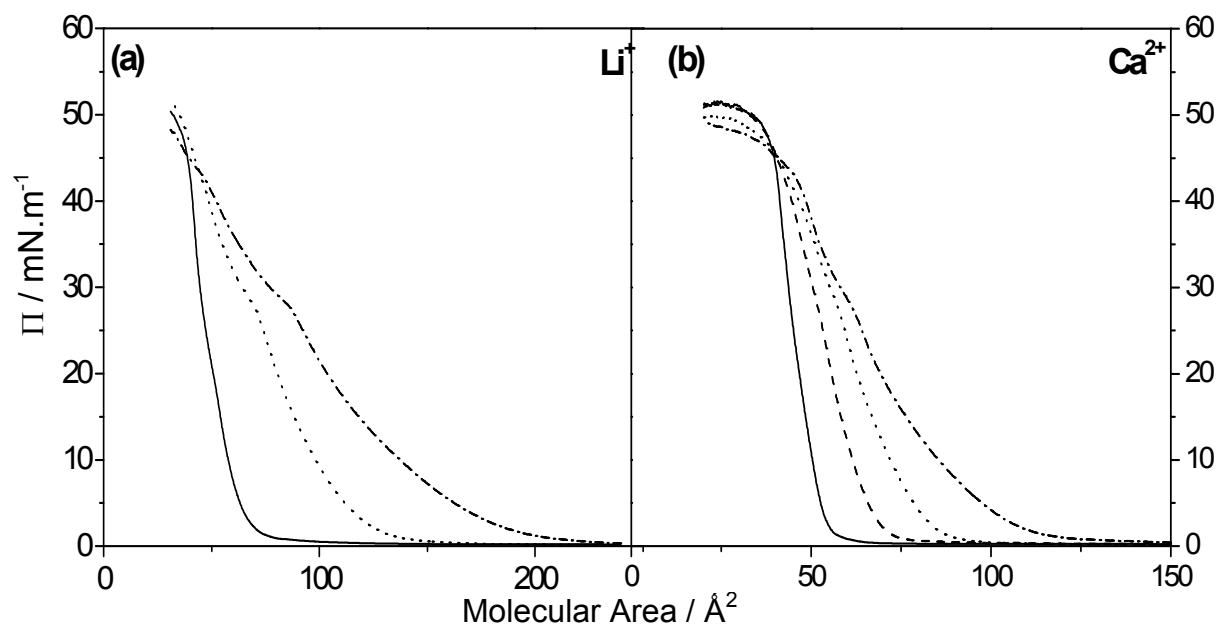


Figure 7: C. I. Cámara, M. V. Colqui, N. Wilke, A. Jimenez-Kairuz and L. M. Yudi.

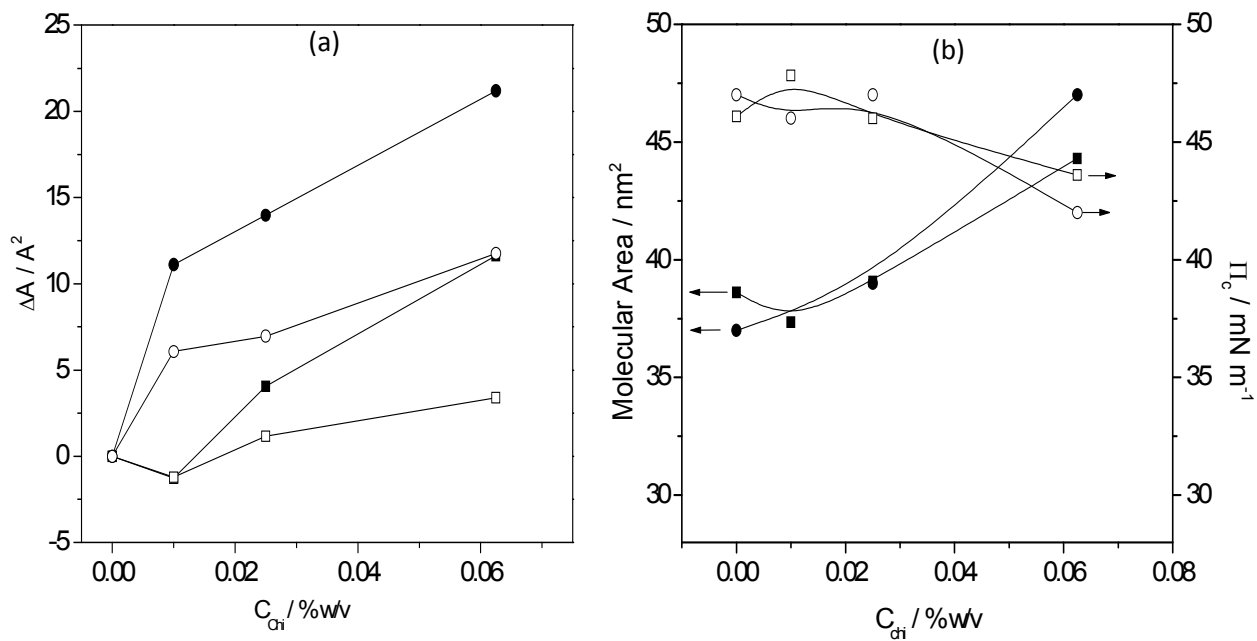


Figure 8: C. I. Cámara, M. V. Colqui, N. Wilke, A. Jimenez-Kairuz and L. M. Yudi.

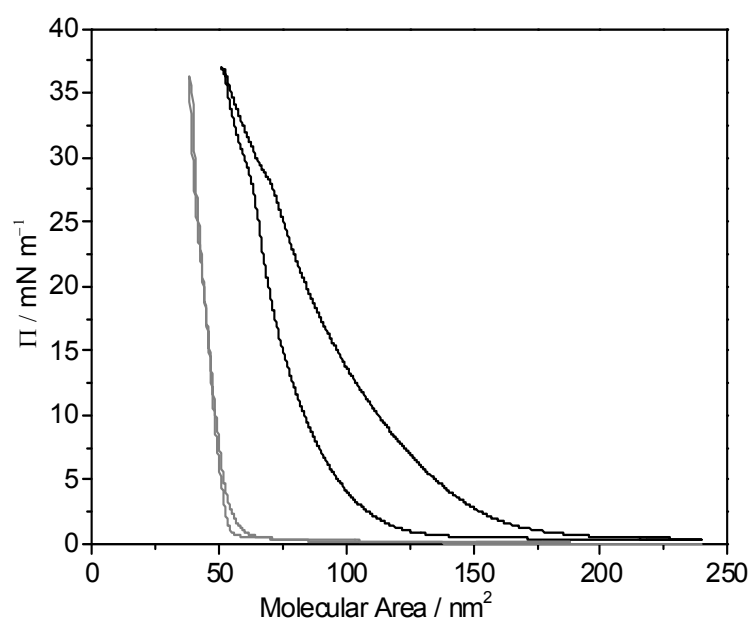


Figure 9: C. I. Cámara, M. V. Colqui, N. Wilke, A. Jimenez-Kairuz and L. M. Yudi

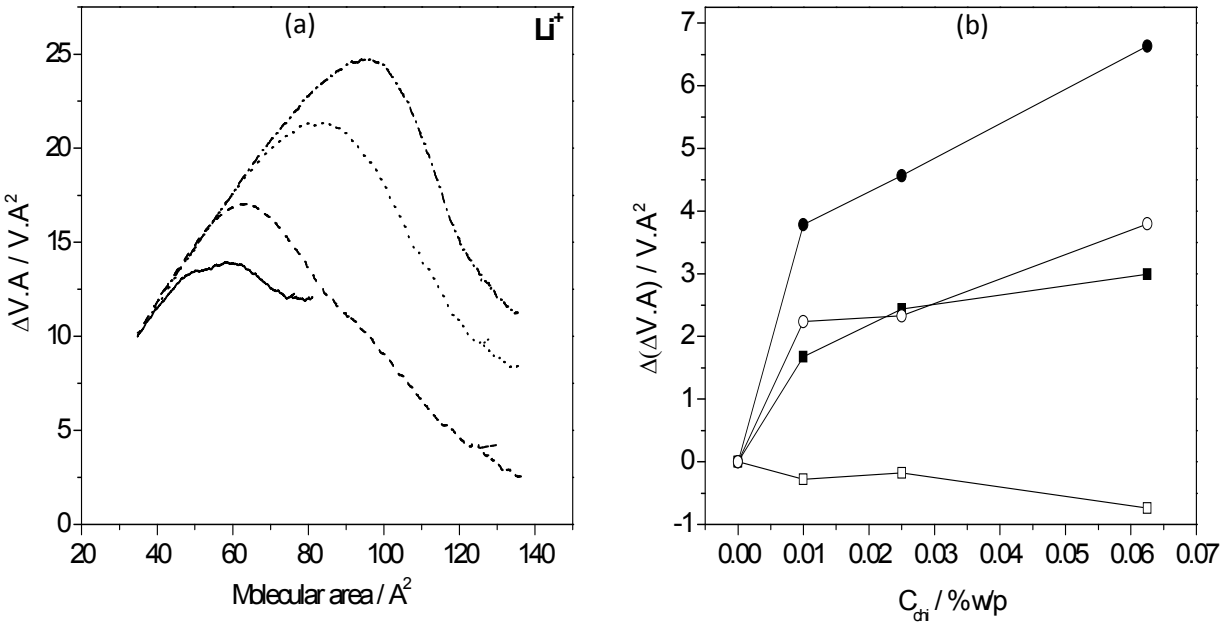


Figure 10: C. I. Cámara, M. V. Colqui, N. Wilke, A. Jimenez-Kairuz and L. M.Yudi

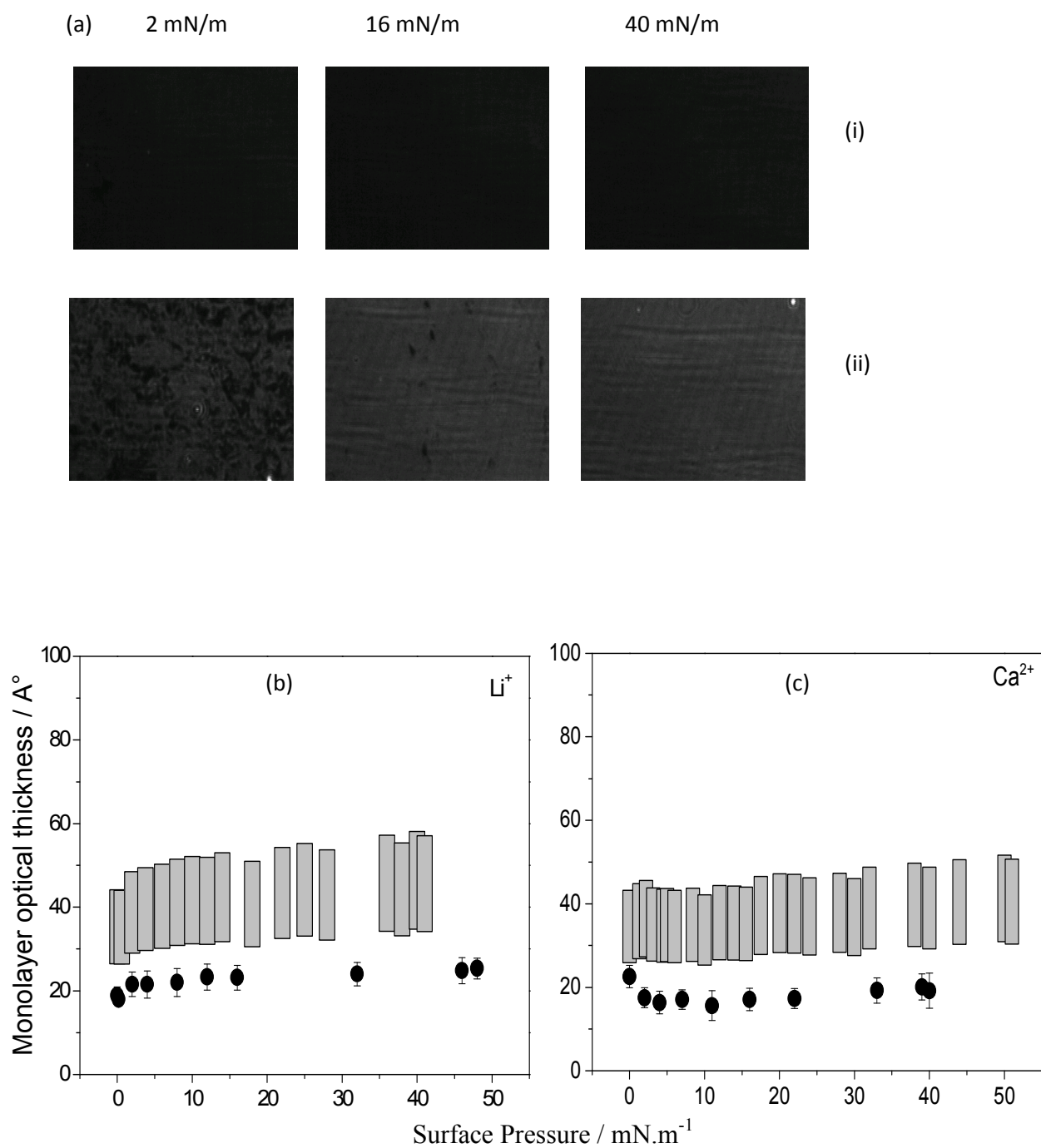
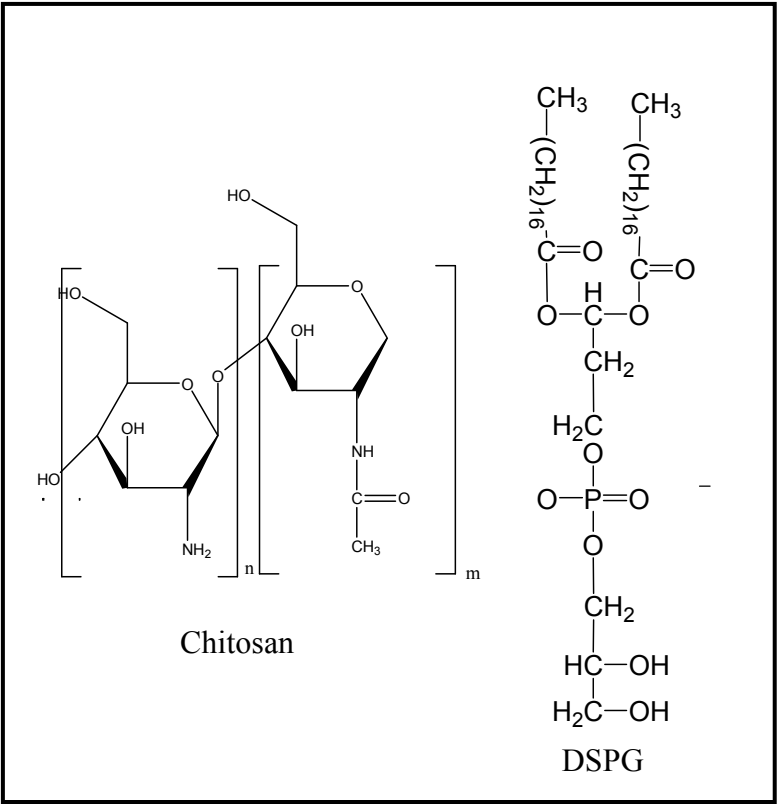
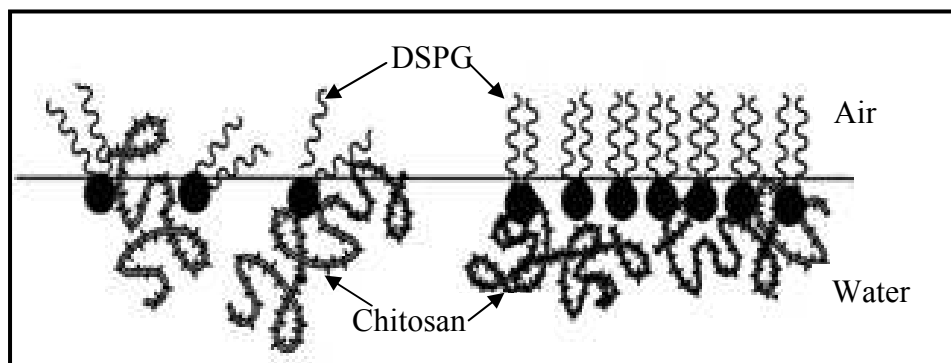


Figure 11: C. I. Cámara, M. V. Colqui, N. Wilke, A. Jimenez-Kairuz and L. M. Yudi

Scheme 1:



Scheme 2:**(a)****(b)**

1
2
3
4
5
6
7
8
9
10
11
12
13
14
15
16
17
18
19
20
21
22
23
24
25
26
27
28
29
30
31
32
33
34
35
36
37
38
39
40
41
42
43
44
45
46
47
48
49
50
51
52
53
54
55
56
57
58
59
60

Table 1:

[C_{chit}]	η x 10⁻⁴	D x 10⁻⁶
% w/p	Pa.s⁻¹	cm².s⁻¹
0	7.13	7.51
0.05	11.20	6.23
0.07	12.50	5.69
0.10	17.60	5.28
0.15	21.50	4.64
0.25	26.40	3.86
0.50	59.50	3.17
1.00	218.00	3.01

Table 2:

$C_{\text{chit}} / \% \text{ w/v}$	$\kappa / \text{mN.m}^{-1}$	
	LiCl	CaCl ₂
0	117	116
0.01	69	48
0.02	44	42
0.06	26	30

TOC

